

## Role of fluctuations in a snug-fit mechanism of KcsA channel selectivity

D. A. Sthagiri and Lawrence R. Pratt

Theoretical Division, Los Alamos National Laboratory, Los Alamos, NM 87545

Michael E. Paulaitis

Department of Chemical Engineering, Ohio State University, Columbus, OH 43210, USA

(Dated: January 27, 2022)

## I. INTRODUCTION

The KcsA potassium channel belongs to a class of  $K^+$  channels that is selective for  $K^+$  over  $Na^+$  at rates of  $K^+$  transport approaching the diffusion limit [1]. This selectivity is explained thermodynamically in terms of favorable partitioning of  $K^+$  relative to  $Na^+$  in a narrow selectivity filter in the channel. One mechanism for selectivity based on the atomic structure of the KcsA channel [2] invokes the size difference between  $K^+$  and  $Na^+$ , and the molecular complementarity of the selectivity filter with the larger  $K^+$  ion [3]. An alternative view holds that size-based selectivity is precluded because atomic structural fluctuations are greater than the size difference between these two ions [4]. We examine these hypotheses by calculating the distribution of binding energies for  $Na^+$  and  $K^+$  in a simplified model of the selectivity filter of the KcsA channel. We find that  $Na^+$  binds strongly to the selectivity filter with a mean binding energy substantially lower than that for  $K^+$ . The difference is comparable to the difference in hydration free energies of  $Na^+$  and  $K^+$  in bulk aqueous solution. Thus, the average filter binding energies do not discriminate  $Na^+$  from  $K^+$  when measured from the baseline of the difference in bulk hydration free energies. Instead,  $Na^+/K^+$  discrimination can be attributed to scarcity of good binding configurations for  $Na^+$  compared to  $K^+$ . That relative scarcity is quantified as enhanced binding energy fluctuations, and is consistent with predicted relative constriction of the filter by  $Na^+$ .

A tetrameric constellation of four TTVGYG amino acid sequences comprises the selectivity filter shown in Fig. 1. This  $K^+$  signature sequence is strongly conserved across a variety of  $K^+$  channels [2]. In each binding site, for example the site defined by  $(VG)_k$ , the ion is coordinated by four carbonyl oxygens from above and four from below. This binding site provides a snug fit for  $K^+$ . Thus it is argued that when  $K^+$  enters the binding site its dehydration is compensated by favorable interactions with the carbonyl oxygens [2, 6, 7]. In contrast, the smaller  $Na^+$  ion is unable to interact optimally with all of the available carbonyls. This imperfect compensation of dehydration is suggested as the basis for the observed selectivity. Implicit in this hypothesis is the idea that the

channel is stiff, and poor coordination of all the carbonyl oxygens leads to weaker binding of the ion to the binding site. We will refer to this as the snug-fit mechanism.

A focused attempt to evaluate the snug-fit mechanism at a molecular level is the recent work of Noskov et al. [4]. They argued that size-based selectivity is precluded because atomic structural fluctuations are greater than the difference in Pauling radii for the two ions. Through numerical experimentation involving extensive free energy calculations, they concluded that local interactions leading to structural flexibility of the binding site provided a key to selectivity for  $K^+$ . They pointed-out that the selectivity of the binding site is sensitive to carbonyl-carbonyl repulsive interactions. Artificially turning-off carbonyl-carbonyl electrostatic repulsion while retaining carbonyl-ion electrostatic attractions was found to shift the thermodynamic selection in favor of  $Na^+$ .

In the analysis below we follow Noskov et al. [4] in studying a simplified model of the selectivity filter. A distinction of the present work with that of Noskov et al. is the use of more parsimonious statistical thermodynamic analyses. This sharpens the physical points that may be observational. On this basis we might expect experimental validation of the key result of these analyses, i.e., that constriction of the filter and enhanced fluctuations accompany each other in the binding of an under-sized ion such as  $Na^+$ . Further experimental investigation of the joint association of these factors might help to clarify the combined roles of fluctuations and a snug fit [2, 4] in the mechanism of ion selectivity by the KcsA channel.

## II. THEORY

The equilibrium selectivity of the filter can be characterized by the difference in the interaction free energy for transferring a  $Na^+$  ion from water into the selectivity filter compared to the case for a  $K^+$  ion. Thus we study

$$\Delta \mu_{Na^+/K^+}^{ex} = \left[ \mu_{Na^+}^{ex}(\text{filter}) - \mu_{K^+}^{ex}(\text{filter}) \right] - \left[ \mu_{Na^+}^{ex}(\text{aq}) - \mu_{K^+}^{ex}(\text{aq}) \right] \quad (1)$$

Here  $\mu_X^{ex}(\text{aq})$  ( $X = K^+, Na^+$ ) is the hydration free energy of the ion, and  $\mu_X^{ex}(\text{filter})$  is the analogous quantity in the selectivity filter.  $\mu_X^{ex}(\text{aq})$ , the excess chemical potential, is that part of the chemical potential that would vanish if intermolecular interactions were to be neglected. Thus,

$x^{ex}(\text{aq})$  is understood to be referenced to the ideal gas result at the same density and temperature. This technical point deserves emphasis because we could adopt a standard state in which  $x^{ex}(\text{aq})$  would vanish, but that would not change any physical consideration.

The potential distribution theorem [8, 9]

$$e^{x^{ex}} = \frac{Z}{e^{h^i} P_X(\epsilon) d\epsilon} = h^i \quad (2)$$

tells us how  $x^{ex}$  may be calculated. Here  $\epsilon$  is the binding energy of the  $X$  ion to the medium;  $P_X(\epsilon)$  is the probability density function of this interaction energy.  $P_X(\epsilon)$  is generated with the ion and the medium fully coupled at temperature  $T = 1/k_B$  where  $k_B$  is Boltzmann's constant. In the present approach ion positions contributing to the sample are those corresponding to its natural motion in the ion-protein system. If  $P_X(\epsilon)$  is well-described by a gaussian of mean  $h^i$  and variance  $\sigma^2 = (\epsilon - h^i)^2$ , then  $P_X(\epsilon) / e^{(\epsilon - h^i)^2 / 2\sigma^2}$ , and

$$x^{ex} = h^i + \sigma^2 = 2 \quad (3)$$

The width parameter gauges a fluctuation contribution.

Note that in sampling the fully-coupled system the term  $\sigma^2 = 2$  raises the chemical potential above the mean binding energy  $h^i$ . This should be contrasted with the case of sampling from the uncoupled subsystems. In the uncoupled case, contributions beyond a mean field term lower the free energy. The distinction reflects the fact that the mean binding energies are computed from different probability distributions.  $P_X^{(0)}(\epsilon)$  is the probability distribution function for the binding energy when the ion and the medium are uncoupled, and is given by

$$P_X^{(0)}(\epsilon) = e^{(\epsilon - x^{ex})} P_X(\epsilon) \quad (4)$$

Intrinsic fluctuations of binding energies are associated with these probability distributions, and contribute to the free energies in a natural way,

$$\begin{aligned} h^i &= \frac{Z}{e^{x^{ex}}} \int \epsilon P_X(\epsilon) d\epsilon \\ &= \frac{Z}{e^{x^{ex}}} k_B T \int \epsilon P_X(\epsilon) \ln \frac{P_X(\epsilon)}{P_X^{(0)}(\epsilon)} d\epsilon \quad (5) \end{aligned}$$

which uses Eq. 4. Here the additional fluctuation contribution, the right-most term in Eq. 5, suggests an entropic contribution to the free energy of binding beyond the mean interaction energy for the joint system. Note specifically, however, that  $h^i$  is expected to be temperature dependent so that this additional fluctuation contribution is not an identification of the thermodynamic entropy contribution.

Additional physical perspective can be obtained from the formal relation

$$x^{ex} = kT \ln \int e^{\epsilon} P_X(\epsilon) d\epsilon - kT \ln \int e^{\epsilon} P_X^{(0)}(\epsilon) d\epsilon \quad (6)$$

which is true independently of the binding energy cutoff parameter  $\epsilon$ ; see for example [8, 10]. We expect  $P_X(\epsilon)$  to be concentrated near  $h^i$ , and thus it is natural to choose  $\epsilon$  so that

$$h^i = kT \ln \int e^{\epsilon} P_X(\epsilon) d\epsilon \quad (7)$$

Then

$$\frac{x^{ex} h^i}{kT} = \ln \int e^{\epsilon} P_X^{(0)}(\epsilon) d\epsilon \quad (8)$$

The natural estimate is  $x^{ex} = h^i$ .

To the extent that the gaussian estimate Eq. 3 is accurate, the observed variance of binding energies observed for the fully coupled system teaches us about available states of the  $X$  ion alone. Fig. 2 illustrates this connection between the available states for the uncoupled selectivity  $X$  ion and the observed fluctuations for the fully coupled system.

We anticipate results that follow by noting that  $\sigma^2 = 2$  takes values ranging from 12 kcal/mol to 6 kcal/mol, roughly, for the cases of  $\text{Na}^+$  to  $\text{K}^+$ . In fact,  $\sigma^2$  will be substantially lower for  $\text{Na}^+$  than for  $\text{K}^+$ . The physical interpretation from Eq. 8 is that we would need sample sizes as big as

$$\frac{1}{R \int e^{\epsilon} P_X^{(0)}(\epsilon) d\epsilon} = \exp\left[-\frac{x^{ex} h^i}{kT}\right] \quad (9)$$

5	$10^8$ ;	$(\text{Na}^+)$ ;
2	$10^4$ ;	$(\text{K}^+)$

to find a  $X$  ion conformation that provides a binding energy  $\epsilon = h^i$  by sampling from uncoupled systems. If we found one favorable conformation in such samples, the probabilities would be all correct. Conformations of the uncoupled  $X$  ion that would be favorable for  $\text{Na}^+$  are thus less probable than those that would be favorable for  $\text{K}^+$ .

As a check for the gaussian approximation Eq. 3, we have also computed  $x^{ex}(X)$  by transforming  $\text{K}^+$  to  $\text{Na}^+$  on the basis of a coupling-parameter integration through 20 intermediate states. This is, of course, a simple algorithmic approach to evaluation of Eq. 2. Note that by introducing multiple gaussians [11], the single gaussian approximation can be refined to achieve quantitative agreement with coupling-parameter integration. We do not pursue this point further here in favor of physical clarity.

### III. CALCULATIONS

The atomic coordinates for the protein structure were obtained from the Protein Data Bank (PDB ID: 1BL8

[2]). Only residues 63 to 85 were retained in the simulation model (Fig. 1). Residues 74 to 79 comprise the selectivity filter. Following earlier notation [1], residues 76 (V) and 77 (G) comprise the binding site denoted as  $S_2$ . All our calculations pertain to a single ion located in the  $S_2$  site.

The N-terminal group of each of the four protein chains was acetylated, the C-terminal group was amidated, and all eight carboxylates were ionized. Hydrogen atom positions were built and the structure was energy minimized keeping only the non-crystallographically determined atomic positions free. This initial structure provided the starting point for further simulations.

The heavy atoms outside the selectivity filter experience a harmonic mean field with force constant  $10 \text{ kcal/mole-Å}^2$ , and similarly the heavy atoms of the selectivity filter felt harmonic external forces corresponding to  $k = 10, 5, 2.5 \text{ kcal/mole-Å}^2$ . We also considered a hybrid case in which  $k = 0.0$  for the carbonyl oxygens of the  $S_2$ , but  $k = 2.5$  for all other atoms of the filter; this is plotted as  $k = 0.0$  in Fig. 6.

Molecular dynamics studies were carried out with the NAMD program [12] using the CHARMM 27 [13] force-field. A temperature of 298 K was maintained by velocity scaling. The Lennard-Jones parameters for the ions were from [14]. All the non-bonded interactions were switched off from 17 Å to 20 Å. A shorter cutoff does not affect the results.

In using Eqs. 2 and 3, we could consider the ion-protein interaction in full. But the binding energy  $\Delta G$  is particularly sensitive to local, near-neighbor interactions, and far-field contributions are expected to be less discriminating between  $\text{Na}^+$  and  $\text{K}^+$  in the filter. Therefore, to obtain differences  $\Delta G^{\text{ex}}(\text{filter})$  we compute only the local interactions between the ions and ligands explicitly present. We investigated several cases for including ion-filter interactions of different types in evaluating the binding energy; our quantitative results changed by about 20% in the extremes, and those different approximations did not affect our conclusions below. For clarity then, we present results for the case where interactions contributing to the binding energy are limited to the carbonyl groups alone. Complementary coupling-parameter integrations with the same scheme for considering interactions were also performed.

For bulk hydration studies, the SPC/E [15] water model was used as much of our preliminary work had been done with this water model. The ion parameters had been developed for the TIP3P water model, but the hydration results with SPC/E are not significantly different. The experimental partial molar volume of the ion [16] was used to fix the simulation volume. For aqueous simulations, long range electrostatics were treated using Ewald summation, with non-electrostatic interactions cutoff at 8.8 Å.

The coupling-parameter transformation of  $\text{K}^+$  to  $\text{Na}^+$  was carried out in 20 steps, with 5 ps (10 ps for aqueous runs) for equilibration and 20 ps for statistical averaging.

For calculations using the gaussian model Eq. 3, a simulation length of 0.5 ns was used and the data stored every 20 steps (25 steps for aqueous runs) for analysis.

## IV. RESULTS AND DISCUSSION

### A. Bulk hydration

The bulk hydration free energies set the baseline for filter selectivity as is evident in Eq. 1. The coupling-parameter integration yields  $\Delta G^{\text{ex}}(\text{aq}) = 20.7$ , in good agreement with [14]. The gaussian model gives  $23.0 \text{ kcal/mole}$ . This result is reasonable for a single gaussian description of aqueous hydration [11], and is consistent with the coupling-parameter integration result.

From Eq. 1, the relative selectivity is  $\Delta G^{\text{ex}}(\text{filter}) + 20.7 \text{ kcal/mole}$ . It is estimated that  $\Delta G^{\text{ex}}(\text{filter})$  is about  $6 \text{ kcal/mole}$  [4], which is about three times smaller than the difference in bulk hydration free energies. Thus the hydration thermodynamic properties in bulk aqueous solution alone play a dominating role in the filter selectivity.

### B. Filter results

Fig. 3 shows the ion-carbonyl oxygen pair distribution function. Notice that carbonyl oxygen atoms approach the  $\text{Na}^+$  more closely, consistent with the smaller size of  $\text{Na}^+$  and the more favorable coulombic interactions obtained then. The carbonyl oxygens are also more delocalized in the case of  $\text{Na}^+$  than that of  $\text{K}^+$ . These observations imply that the selectivity filter has conformational flexibility to readily accommodate  $\text{Na}^+$ , as opposed to the static structural picture discussed in standard texts, for example Fig. 13.25 in [17] and Fig. 11.24 in [18], in which the ion moves about within a fixed filter structure. Instead these results suggest that the  $\text{Na}^+$  would achieve favorable binding energies by shifting the ensemble of configurations for the filter away from that for the case of  $\text{K}^+$ .

This relative constriction can be directly observed as Fig. 4 shows. This narrowing is expected to be sensitive to the repulsive interactions between carbonyl-oxygen atom pairs which have been implicated in selectivity [4]. But selective manipulation of carbonyl O-O repulsions is artificial and, thus, experimental investigation of the necessity of this point does not seem likely.

Fig. 5 shows the distribution of ion-carbonyl binding energies for the  $k = 0$  case. It is clear that the mean interaction energy of  $\text{Na}^+$  with the filter is much lower than for  $\text{K}^+$ . In addition, the distribution of this interaction energy for  $\text{Na}^+$  is broader than that for  $\text{K}^+$ , consistent with relative widths of the distributions of Fig. 3.

Fig. 6 collects the results for the various cases considered. These results are not importantly sensitive to  $k$ .

Consistent with experiments,  $\Delta G^{\text{ex}} > 0$ : the filter selects  $K^+$  over  $Na^+$ . The magnitude of  $\Delta G^{\text{ex}}$  is also roughly consistent with the estimate of about 5–6 kcal/mole [4].

Nevertheless,  $Na^+$  achieves the energetically more-favorable binding to the filter. *h*"i, the difference in mean binding energy of  $Na^+$  to the filter relative to that for  $K^+$ , is between 22 kcal/mole and 25 kcal/mole, consistent with the energy difference noted in [4]. These values are about the same as the difference in aqueous hydration free energy of 23 kcal/mole. Thus, filter discrimination against  $Na^+$  on the basis of binding energies alone is implausible.

However, the difference in fluctuation contributions, ( $\Delta G^{\text{fluc}} \approx 2$ ), must also be considered, and the magnitude of this difference is comparable to the net selectivity, as Fig. 6 shows. ( $\Delta G^{\text{fluc}} \approx 2$ ) is roughly 5–6 kcal/mole, indicating that filter conformations conducive to binding  $Na^+$  are comparatively rare, consistent with Eq. 9. It is this difference in fluctuation contributions for  $Na^+$  relative to  $K^+$  that shifts the balance in favor of  $K^+$ .

## V. CONCLUSIONS

$Na^+$  binds strongly to the selectivity filter with a mean binding energy substantially lower than for  $K^+$ . The difference is comparable to the difference between the hydration free energies for these two ions in bulk aqueous solution. Since the ion-sorting ability of the KcsA  $K^+$  filter must be considered from the baseline of this substantial difference in bulk hydration free energies, we conclude that the average filter binding energies alone do not provide significant discrimination of  $Na^+$  from  $K^+$ .

Strong binding of the smaller  $Na^+$  also constricts the selectivity filter. From the point of view of the filter, discrimination against  $Na^+$  results from the fact that the observed  $Na^+$ -narrowed conformations are rare occurrences in the ensemble of conformations favorable to  $K^+$ . This effect is described in the thermodynamics as an observed fluctuation contribution that is destabilizing for  $Na^+$  relative to  $K^+$ . The key result here is the association in the

case of  $Na^+$  of strong binding, constriction of the filter, and enhanced fluctuations.

With respect to the snug-fit view of channel selectivity, it is clear that a favorable binding energy is important. In the case of the smaller ion ( $Na^+$ ), this is achieved at the expense of stronger energetic and positional (Fig. 4) fluctuations. For the ion considered to have the better geometrical fit ( $K^+$ ), this is achieved at a lower cost in energetic and positional fluctuations. In this sense, the size difference between  $Na^+$  and  $K^+$ , and the molecular complementarity of the selectivity filter with  $K^+$  do play a role in channel selectivity. From the fluctuations point of the view, the idea of a pre-conformed empty channel is hypothetical. Conformational flexibility induced by strong binding of the smaller  $Na^+$  in the selectivity filter is central to the mechanism of  $Na^+$  discrimination.

This work supports the view that selectivity can be addressed by analysis of local interactions involving a single-ion binding site [4]. The assessment of rates, though, likely requires an account of interactions between ions occupying different channel binding sites [9], but fluctuations of the sort identified here probably play a role too.

The identification of channel-reorganization (induced fit) fluctuations is suggestive of solvent reorganization in chemical dynamics. The fact that a simple distribution, gaussian with slight positive skewness as in Fig. 5, works satisfactorily will have important conceptual and practical consequences for modeling aqueous electrolyte solutions more broadly.

## Acknowledgements

This work was supported by the US Department of Energy, contract W-7405-ENG-36, under the LDRD program at Los Alamos. LA-UR-05-4622. Financial support from the National Science Foundation (CTS-0304062) and the Department of Energy (DE-FG02-04ER25626) is gratefully acknowledged.

- 
- [1] Latorre, R. & Miller, C. (1983) *J. Membrane Biol.* 71, 11{30.
- [2] Doyle, D. A., Cabral, J. M., Puetzner, R. A., Kuo, A., Gulbis, J. M., Cohen, S. L., Chait, B. T., & Mackinnon, R. (1998) *Science* 280, 69{77.
- [3] Bezanilla, F. & Armstrong, C. M. (1972) *J. Gen. Physiol.* 60, 588{608.
- [4] Noskov, S. Y., Bemèche, S., & Roux, B. (2004) *Nature* 431, 830{834.
- [5] Heginbotham, L., Lu, Z., Abramson, T., & Mackinnon, R. (1994) *Biophys. J.* 66, 1061{1067.
- [6] Mackinnon, R. (2003) *FEBS Lett.* 555, 62{65.
- [7] Armstrong, C. M. (2003) *Sci STKE* 188, re10.
- [8] Beck, T. L., Paulaitis, M. E., & Pratt, L. R. (in press 2005) The potential distribution theorem and models of molecular solutions Cambridge University Press LA-UR-04-7891.
- [9] Paulaitis, M. E. & Pratt, L. R. (2002) *Adv. Prot. Chem.* 62, 283{310.
- [10] Pratt, L. R. & Asthagiri, D. (2005) Potential distribution methods and free energy models of molecular solutions Technical report Los Alamos Natl. Lab. LA-UR-05-0873.
- [11] Hummer, G., Pratt, L. R., & Garcia, A. E. (1997) *J. Am. Chem. Soc.* 119, 8523 { 8527.
- [12] Kale, L., Skeel, R., Bhandarkar, M., Brunner, R., Gursoy, A., Krawetz, N., Phillips, J., Shinozaki, A., Varadarajan, K., & Schulten, K. (1999) *J. Comp. Phys.* 151, 283.
- [13] Mackerell, Jr., A. D., Bashford, D., Bellott, M., Dun-

- brack Jr., R. L., Evanseck, J. D., Field, M. J., Fischer, S., Gao, J., Guo, H., Ha, S., & Joseph-McCarthy, D. (1998) *J. Phys. Chem. B* 102, 3586{3616.
- [14] Beglov, D. & Roux, B. (1994) *J. Chem. Phys.* 100, 9050 { 63.
- [15] Berendsen, H. J. C., Grigera, J. R., & Straatsma, T. P. (1987) *J. Phys. Chem.* 91, 6269{6271.
- [16] Marcus, Y. (1985) *Ion solvation* Wiley, London.
- [17] Berg, J. M., Tymoczko, J. L., & Stryer, L. (2002) *Biochemistry* W. H. Freeman, New York.
- [18] Alberts, B., Bray, D., Lewis, J., Raff, M., Roberts, K., & Watson, J. D. (2002) *Molecular biology of the cell* Garland Science, New York.
- [19] Zhou, Y. & Mackinnon, R. (2003) *J. Mol. Biol.* 333, 965{975.

## Figures

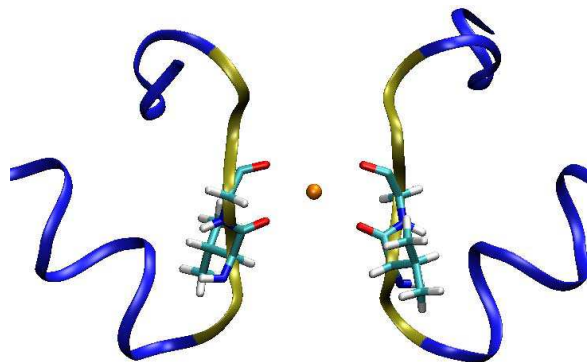


FIG. 1: Depiction of the channel filter. Only two of the four chains are shown for clarity. Heavy atoms in the blue ribbon segment experience a harmonic mean field, i.e., they are "restrained" with spring of force constant  $k = 10 \text{ kcal/mol-Å}^2$ . The segment colored yellow is the TVGYG sequence of amino acids comprising the selectivity filter. The  $S_2$  site defined by VG is shown with the bound ion.

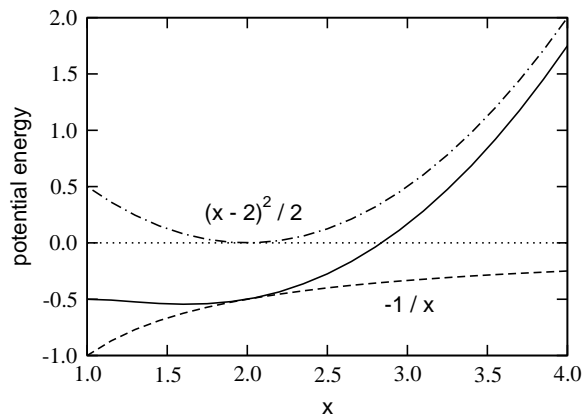


FIG. 2: An example how coupling an ion and the filter might enhance fluctuations. Here a coordinate in a parabolic potential-energy well also experiences a coulombic attraction displacing the minimum energy position leftward (unbroken line). The fluctuations observed for the fully-coupled system, corresponding to the potential energy function given by the solid curve, characterizes the available states on the harmonic potential function in the neighborhood of the physical binding energies. The curvature at the minimum is reduced, fluctuations are enhanced, and the observed fluctuations raise the free energy above the mean binding energy, according to Eq. 3.

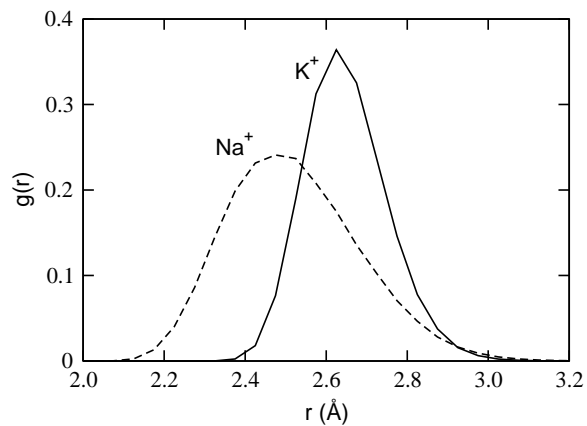


FIG .3: Normalized distribution of carbonyl oxygens radially from the ion, for the  $k = 0$  (hybrid) case described in the text for the wild type (bold lines) and the (GG) mutant (lighter lines). Notice that the longest ion-oxygen distance is about the same in each case, but the shortest ion-oxygen distances, and the most probable ones, are shorter in the case of  $\text{Na}^+$ . This suggests that  $\text{Na}^+$  isn't merely delocalized, but constricts the filter relative to the  $\text{K}^+$  case.

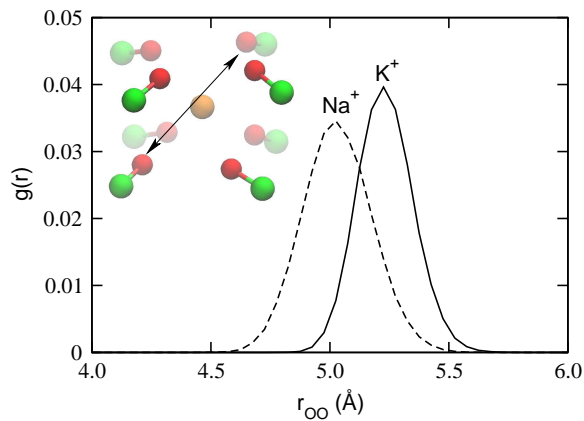


FIG .4: Normalized radial distribution of body-diagonal  $\text{OO}$  pairs, indicated by the arrow, for the selectivity filter in the cases of  $\text{Na}^+$  and  $\text{K}^+$ , indicating relative constriction of the filter by  $\text{Na}^+$ . Bold lines: wild type. Lighter lines: (GG) mutant. Inset: atoms of the selectivity filter, showing an example of the  $\text{OO}$  body-diagonal. Carbonyl oxygen atoms are in red, carbonyl carbons are green, and the ion is orange. Notice that the width of the distribution for the  $\text{Na}^+$  case is slightly the larger, and that relative widths,  $\text{width} = r_{\text{max}}$ , of these distributions are roughly 10%.

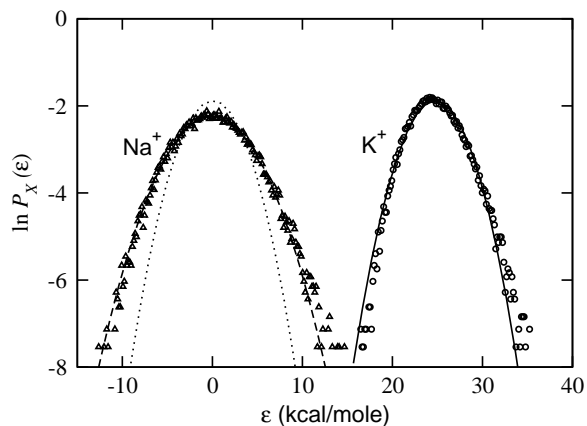


FIG. 5: Normalized distribution of ion carbonyl binding energies for the  $k = 0$  case for the wild-type. The circles ( $K^+$ ) and triangles ( $Na^+$ ) are the raw data. The binding energy abscissa is measured relative to the mean binding energy,  $\langle \epsilon \rangle$ , for the  $Na^+$  case. Thus, the mean binding energy for  $K^+$  is about 22-25 kcal/mol higher than for  $Na^+$ . Gaussian fits to the data are smooth curves, and the additional dotted line on the left superposes the fit for the  $K^+$  case on the  $Na^+$  data. This shows that the distribution is distinctly broader for the  $Na^+$  case. Similar results are obtained for the  $k = 10; 5.0; 2.5$  cases.

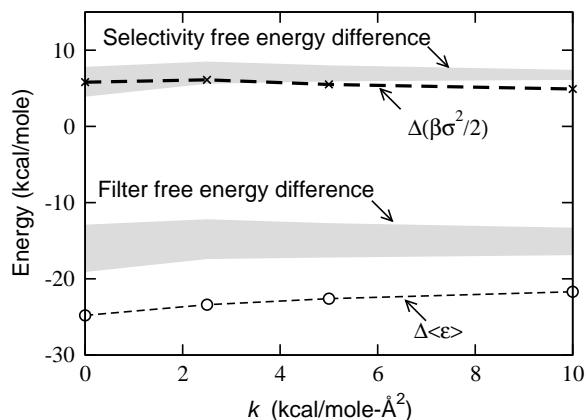


FIG. 6: Free energy results for several values of the force constant  $k$  used in the harmonic mean field. The lower gray band is  $\Delta \langle \epsilon \rangle$  (filter) of Eq. (1). The upper gray band is  $\Delta \langle \beta \sigma^2 / 2 \rangle$ , the left-side of Eq. (1). The lower boundary of each gray band is the result of the gaussian model Eq. 3, and the upper boundary was obtained on the basis of coupling-parameter integration. Note that the mean interaction energy differences (circles) are negative, signifying the better interaction of  $Na^+$  with the channel.